Field Measurements of a Full Scale Tidal Turbine

Penny Jeffcoate[a], Ralf Starzmann[b], Bjoern Elsaesser[a], Stefan Scholl[b], Sarah Bischoff[b]

[a]*Queen's University Belfast, Stranmillis Road, Belfast BT9 5AG, p.jeffcoate@qub.ac.uk (Corresponding author) +44 (0) 28 9097 4012*

[b]*SCHOTTEL – Josef Becker Forschungszentrum GmbH, Mainzer Straße 99, 56322 Spay/Rhein, Germany, RStarzmann@schottel.de*

Abstract

Field testing studies are required for tidal turbine device developers to determine the performance of their turbines in tidal flows. Full-scale testing of the SCHOTTEL tidal turbine has been conducted at Queen's University Belfast's tidal site at Strangford Lough, NI. The device was mounted on a floating barge. Testing was conducted over 48 days, for 288 hours, during flood tides in daylight hours. Several instruments were deployed, resulting in an expansive data set. The performance results from this data set are presented here. The device, rated to 50kW at 2.75m/s was tested in flows up to 2.5m/s, producing up to 19kW, when time-averaged. The thrust on the turbine reached 17kN in the maximum flow. The maximum system efficiency of the turbine in these flows reached 35%. The test campaign was very successful and further tests may be conducted at higher flow speeds in a similar tidal environment.

Keywords: Tidal energy, tidal turbines, full-scale, field testing, performance assessment

Nomenclature and Abbreviations

ADP	Acoustic Doppler Profiler
ADV	Acoustic Doppler Velocimeter
C_T	Coefficient of Thrust
d	Depth
d_h	Hub depth
D_E	Equivalent Diameter
n	Rotation rate
P_{el}	Electrical Power
PTO	Power Take-Off
RPM	Rotations per Minute
STG	SCHOTTEL Tidal Generator
T	Thrust
TEC	Tidal Energy Converter
TSR	Tip Speed Ratio
U_{in}	Inflow velocity
$\eta_{system,i}$	System efficiency

1. Introduction

The development of tidal energy converters and the advancement from lab-scale tests to prototype devices has accelerated in recent years. Many devices have been tank tested at model scales, such as Scotrenewables 1/40 to 1/7 scale tests [1] and Oceanflow 1/40 scale tests [2], and several have been deployed as full-scale devices; some examples of these are Andritz Hydro Hammerfest HS1000 [3], Alstom TGL DeepGen [4], Marine Current Turbines SeaGen [5], Verdant Power KHPS [6], Atlantis Resources AR1000 [7] and Scotrenewables SR250kW [8]. One of the key features for device developers to understand is how their turbine performs in 'real' turbulent tidal flows compared to laboratory flows [9]. This can be assessed by deploying a medium- or full-scale device in tidal field studies.

Queen's University Belfast recently conducted a series of experiments to determine the effect of tidal flows on 1/10 scale devices [10], as well as testing the scale models of Oceanflow's Evopod device [2], and in doing so developed a tidal test centre in Strangford Lough, which has flow speeds up to 2.5m/s. SCHOTTEL also recently conducted model scale towing tank tests as well as pushing tests of their full-scale device [11] and wished to develop their understanding of the turbine's performance in tidal flows at full-scale.

During the summer of 2014, Queen's University Belfast, SCHOTTEL and Fraunhofer IWES collaborated under the EU MaRINET project to conduct a series of field tests of a full-scale tidal turbine in highly turbulent flows in Strangford Lough, N.I. The full scale device, the SCHOTTEL Tidal Generator (STG), was designed and constructed by SCHOTTEL and deployed at the QUB tidal test facility from June through to September. The 4m turbine, rated at 50kW, operates from flow speeds of 0.8m/s and reaches maximum power at 2.75m/s, so was operational at the QUB site. The turbine characteristics, inflow conditions and loading on the structure and rotor were all measured and used to calculate the performance characteristics of the turbine.

The testing method and turbine performance characterisation were guided by the IEC62600-200 Technical Specification for Tidal Energy Converter (TEC) power performance assessment [12]. Several parts of the IEC TS standard were used for reference, particularly in terms of data processing, though there were several sections that differed from the testing performed. The TS is useful as a tool because it provides guidelines on techniques such as device placement, filtering and depth-averaging velocities, along with many testing methods. The main advantages of using the TS is that it gives a good basis for testing methods and data analysis techniques employed, and it also allows different devices to be directly compared in terms of site characteristics, turbine performance and operation. There are specific requirements for reporting the site conditions; however, this paper will focus on the turbine performance and output, rather than the site itself. Clauses of the TS used will be indentified in the text.

The key objectives of this paper are: to present a vessel-mounted testing method for field studies of medium- and full-scale tidal devices; to investigate the performance of a full-scale device in tidal flows; and to apply the IEC standards to data processing. This paper details:

the tidal field site characteristics; the turbine description; the full-scale field testing method and equipment at the tidal field site; and the measured turbine performances.

2. Site and test conditions

The QUB tidal site in Strangford Lough is along the Eastern shore of Strangford Narrows. The test vessel, a dump barge, was moored at approximately 54°22.9N 005°33.3W [13], shown in Figure 1. The depth contours of the site are shown; however, for clarity of the plateau where the mooring was located the contours are limited to 30m depth. The deepest part of the channel reaches 60m.

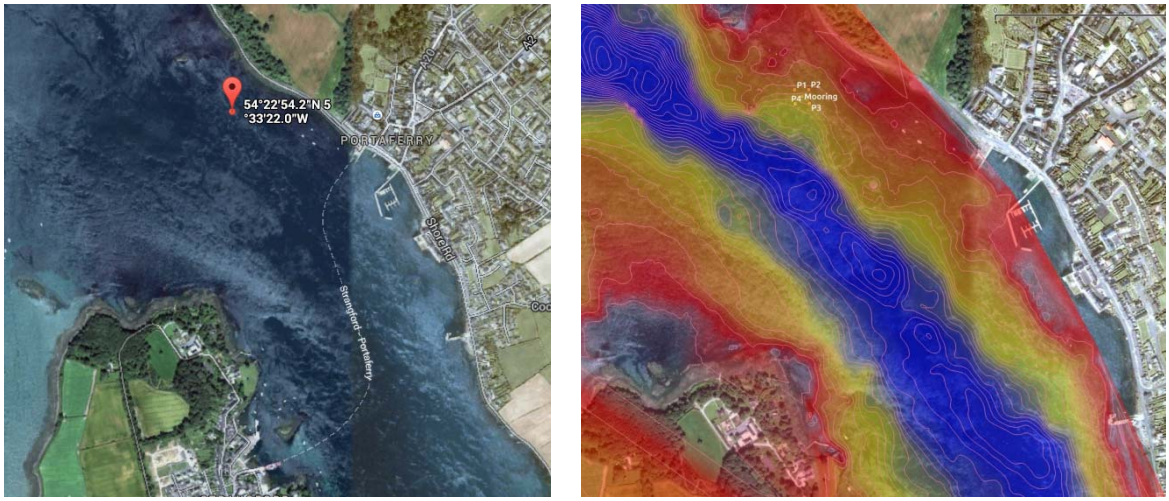

Figure 1: Location of mooring – left: Lat/Lon, right: Depth contours (blue -30m, red 0m)

The lowest astronomical tide (LAT) with respect to chart datum on Admiralty Chart 2159 is 10m; however, the bed contour resolution is low so the depth was independently checked using barge mounted sonar. Using sonar data the lowest tide height at springs during the test period was 9.6m. The maximum water depth recorded was 15.8m. The range at the site was not however 6.2m; the barge was attached to a mooring that allowed it to swing over different parts of the bed depending on the tide (i.e. slack water or full flow) and wind direction. It can also be noticed that the depth to chart datum varies by 4m over the tracks, hence the large range in sonar depth recordings.

Three example tracks of the barge movement are shown in Figure 2. These show that the barge swings about the mooring during the ebb and flood tides. A small amount of the ebb is shown on these plots and the movement during Low Water can be seen. The mooring extends out during ebb flow, and then moves towards the centre of the track during slack water, when there is no thrust on the mooring. Once the turbine was operational and the flood tide accelerated the mooring extended in the opposite direction. This also shows that the main flow direction during flood tide was 135° and during the ebb tide is 315°. During operation the barge position can swing by up to approximately 20m; this results in variations in the directionality about the mooring of approximately 10°. This means that there can be a 10° variation in the inflow velocity condition at the mooring and at the barge, but since the ADP is mounted on the same vessel as the TEC the incoming velocity recorded is the same as that

that is experienced by the turbine. Also, because the frequency and angle of the oscillations about the mooring is relatively low compared to the fluctuations in the incoming velocity, no correction has been applied for this barge movement.

Mounting the ADP on the same vessel as the TEC has the added advantage that the pitch, roll and yaw of the vessel, and the extension of the mooring do not need to be accounted for in post-processing, because the ADP and TEC are on the same reference frame. This would be more complex if a bed mounted ADP were used for quantifying the inflow velocity condition. Also, because the depth changes over the tidal cycle, the bins covering the TEC rotor area would change for a bed-mounted ADP, but does not for a vessel-mounted ADP, meaning that data analysis has less inherent errors.

The variation in the depth can, however, have an effect on the inflow conditions in terms of the turbulence intensity, shear profile and depth-averaged velocity. The shear profile will be discussed in a Section 5.2, but unfortunately the differences in the profile cannot be accounted for in this data analysis. Since the ADP and TEC have the same support structure the power-weighted velocity will cover the TEC swept area regardless of depth, but the turbulence intensity may vary. This will be investigated in subsequent analysis and publications.

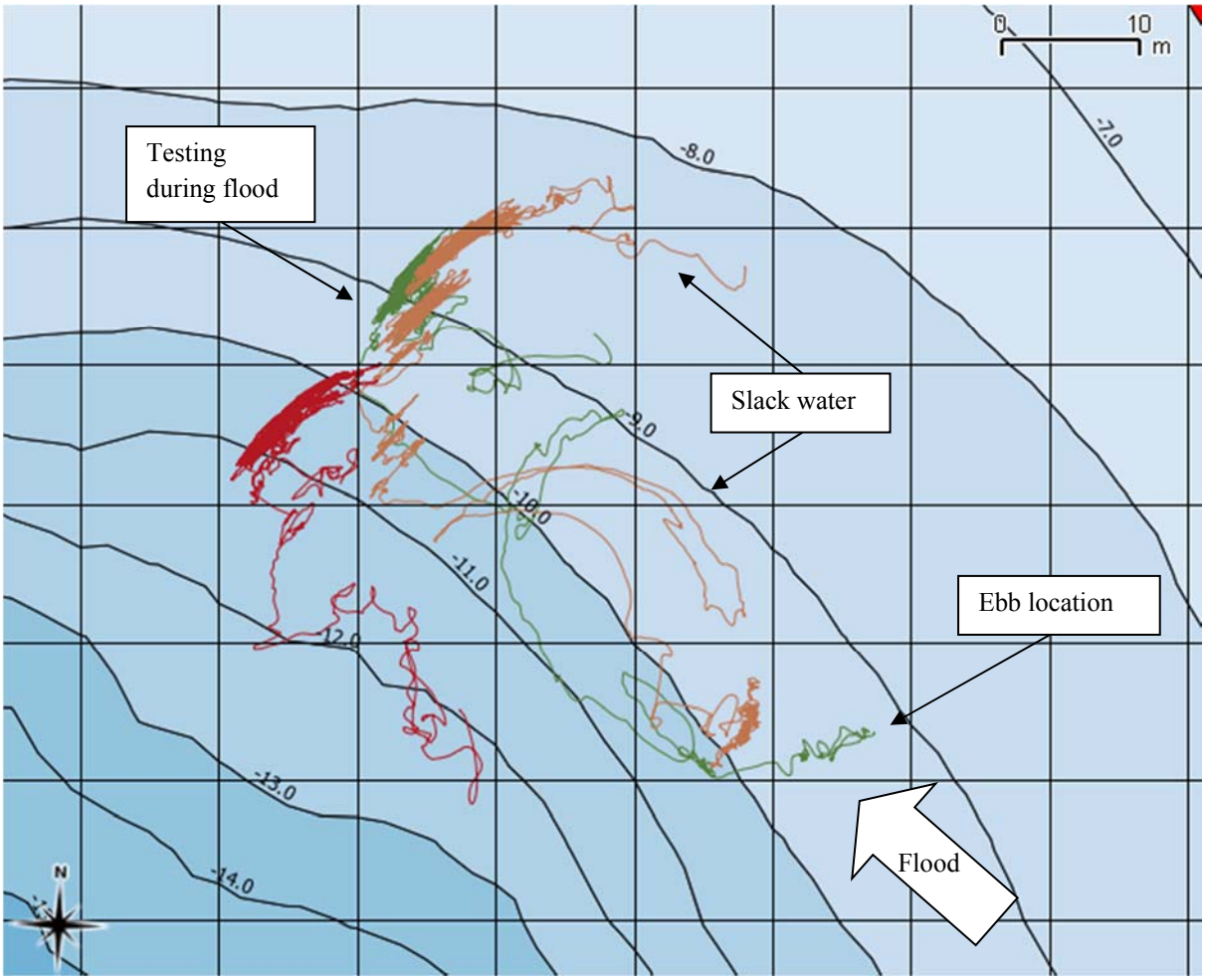

Figure 2: GPS tracks of barge over 3 slack water and flood tides

During the testing period the flood velocities varied from approximately 0.4m/s to 2.5m/s. The flow speed depended on the tide state, the range and the environmental conditions such as the wind and atmospheric pressure; however, there was no detailed recording of these conditions. The flow velocity alone was recorded, but was the correct incoming velocity for the power assessment of the TEC so considered suitable for the analysis. During the ebb tide the velocities did not exceed 1m/s, due to the location of Walter Rock upstream from the site. The tide ebbs either side of the rocks, creating an eddy at the test site location, with some back flow. As a result, testing could only be conducted on the flood tide.

There is minimal wave action at the site, because of the surrounding topography and shelter. The most significant wave action on the testing area is the local ferry wash, which has an approximate wave height of 0.5m. Wave action was therefore not considered in the analysis.

3. Investigated Turbine Design

The STG features a rated electrical power of 50kW, a rotor diameter of 4m at a rated inflow velocity of U_{in} = 2.75m/s. The layout of the STG is simple and robust, avoiding complex subsystems. It consists of a fixed pitch three-bladed rotor, slow speed shaft, planetary gear box and asynchronous generator, both cooled by the flow of ambient water (Fig. 3).

Figure 3: SCHOTTEL Tidal Generator STG - left: CAD model, right: Physical turbine

It has no active pitch mechanism and therefore the control system is very simple: after running at variable speed and capturing optimum power up to rated speed, the turbine goes into controlled overspeed as the flow velocity increases still further. The power taken from the turbine is kept constant while the rotational speed is increased. The general hydrodynamic design of the rotor blades aims for a reduced thrust coefficient, C_T, at higher tip-speed ratios (TSR). To keep thrust forces in overspeed conditions low, passive-adaptive rotor blades out of carbon-fibre have been developed, as proposed by Nicholls-Lee [14] for example. These flex in overload conditions so that the pitch angle of the blades increases and the thrust forces are limited. This keeps the loads on the turbine, and especially on the support structure, low. Moreover, the cavitation inception can be delayed in overspeed conditions.

Prior to the sea trials, as discussed in this study, full-scale pushing tests as well as model-scale towing tank testing have been carried out to validate the STG blade design [11].

Furthermore, a complete drive-train has been installed in a submerged back-to-back configuration and was subjected to extensive laboratory testing [15]. Two blade sets were used in these tests: the commercial passive-adaptive blades and the rigid blades. These two sets have the same hydrodynamic shape but a different structural design. In conditions below 2.5m/s the blades perform similarly, but in larger flow speeds the passive-adaptive blades reduce maximum power performance attainable but also significantly reduce the loading on the rotor. At the QUB tests site flow speeds do not exceed 2.5m/s, therefore the passive-adaptive quality of the blades is not a necessary requirement. To better compare with smaller-scale, model tests and numerical simulations described in [11] the rigid blade set was used in this study. Further study of the difference between the two blade sets in this tidal environment would be beneficial, but will be focussed on in future tests with higher flow speeds.

Figure 4 shows the main components of the drive train. The drive train consists of an asynchronous machine, so it is necessary to energize the DC-link with an external power source. This external power source was a diesel-electric engine (1) placed on the barge. The turbine was controlled by a frequency inverter (2). Internally the frequency inverter consists of three primary components: the rectifier (3), the output module (4) and the chopper module (5). An on-board controller drives the output module, and therefore the turbine, by setting different speed and torque values. As shown in Figure 4 the frequency inverter is used to drive the generator. The inverter varies the speed of the generator and, therefore, the generator terminal frequency. The inverter decouples the generator from the grid and makes it possible to drive the generator at variable speed. The excitation voltage comes from a DC-link. Since the STG operates with variable sped, a frequency inverter is needed. A three phase choke (7) is connected in-between the output module and the generator to smooth the electrical currents. If a defined threshold value in DC-link voltage is reached (650V) the chopper is activated and the energy is discharged by the load bank (6).

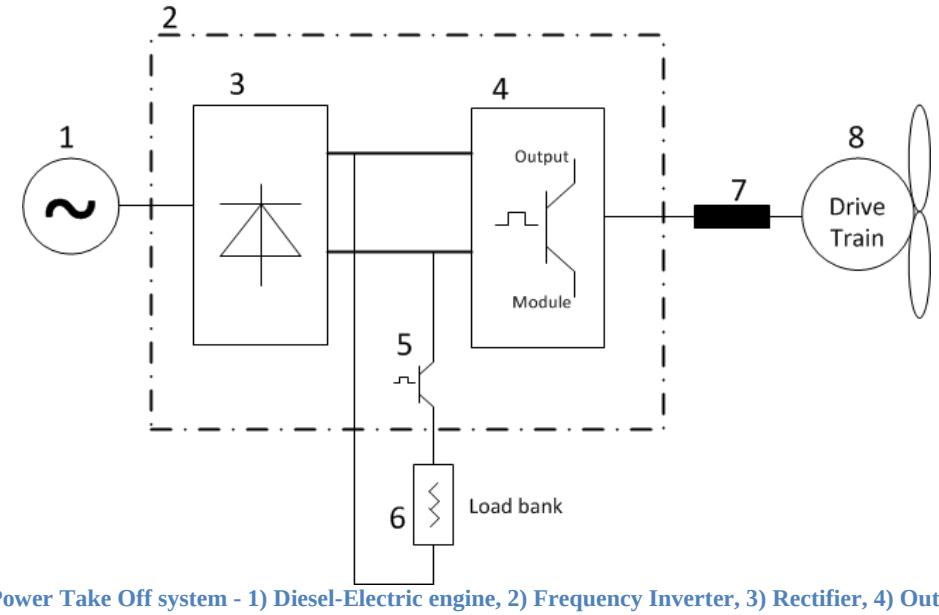

Figure 4: Power Take Off system - 1) Diesel-Electric engine, 2) Frequency Inverter, 3) Rectifier, 4) Output module, 5) Chopper module, 6) Load bank, 7) Chokes, 8) Drive train (Generator, Gearbox and Rotor blades)

A summary of all relevant technical TEC parameters are summarised in Table 1, based on [12, Subclause 6.2].

Table 1: Summary of TEC parameters

TEC make/type	SCHOTTEL STG
TEC diameter [m]	4
TEC serial number	STG-000003
TEC production year	2014
Rated power [kW]	50
Rated velocity [m/s]	2.75
Cut-in velocity [m/s]	0.8
Cut-out velocity [m/s]	6
Rotational speed range [rpm]	15 – 190

4. Experimental Set-up

4.1 Mooring

The mooring used was a 4-point mooring with a riser. The main North and South anchors, which took most of the mooring load, were 1.5ton fluked ship anchors and the East and West anchors were 500kg railway wheels. These were linked to 27.5m chain to a single riser 8m long. Close to the surface the riser was linked to a 6m rope bridle which was attached to the port and starboard sides of the barge bow, described below.

4.2 Barge layout

The STG turbine was mounted on a support frame suspended below a testing barge. The barge was 10m long by 4m wide by 1m high. The barge was 0.35m submerged, giving a total displacement of approx. 14ton. The turbine support was mounted on the stern of the barge and attached to a lifting A-frame. Figures 5 and 6 show the turbine and frame in the testing position and Figures 7 and 8 show the turbine and frame in the lifted position. The sensors used during operation are also shown in Figure 5.

The turbine could be lifted clear of the water (between tests and for checks) and lowered for operation. When lowered the turbine hub was 3.4m below the surface so the blade tips swept an area from 1.4m to 5.4m below the surface. The layout of the equipment on the barge deck is shown in Figure 9.

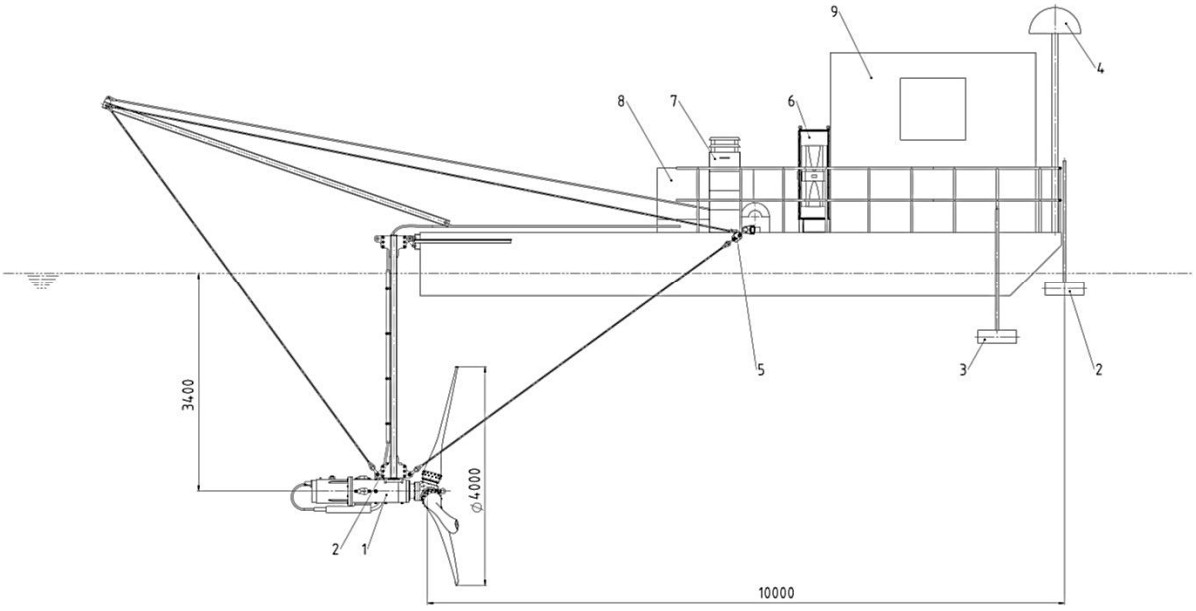

Figure 5: Schematic of barge with turbine in testing position - 1) TEC, 2) ADP, 3) ADV & Sonar, 4) DGPS, 5) Load cell, 6) Electrical Cabinet, 7) Resistor Bank, 8) Generator, 9) Operations Room

Figure 6: Barge with turbine in testing position

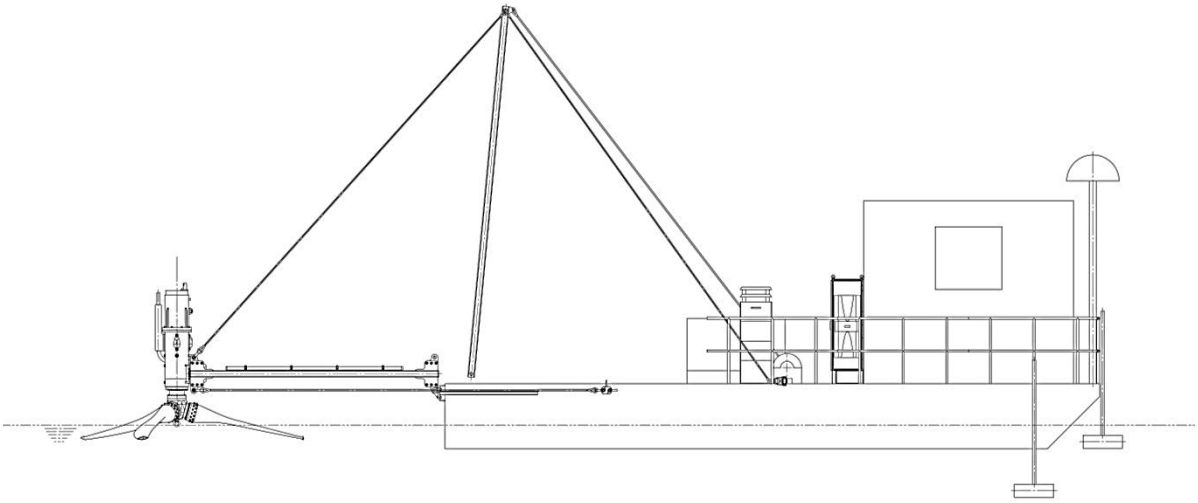

215

216 **Figure 7: Schematic of barge with turbine in lifted position**

217

218

219 **Figure 8: Barge with turbine in lifted position**

Figure 9: Barge equipment layout

4.3 Sensors and data acquisition

There were numerous sensors on the turbine itself, the support frame and on the barge. All of the different sensors used on the barge are outlined below, with their main characteristics and outputs, to show the full scope of the data collection method; however, only some of the sensor measurements are used in this publication. Other data collected will be published in due course.

A control and data acquisition system (6-8) is used to collect instantaneous data from the turbine with a sampling frequency of 10Hz. The electrical power is measured using the response signal from the inverter. A speed sensor measures the rotational speed of the fast running shaft.

Mounted on the support structure there was a Nortek Aquadopp Acoustic Doppler Profiler (ADP, 2) to measure the wake of the turbine at the hub height. This was orientated on the support frame so that a single beam measured the velocity along the x (streamwise) direction into the wake, to record the velocity deficit with distance from the turbine. Also mounted on the support frame were two load cells (5) to record the thrust on the frame and rotor. These were attached to the cables holding the turbine into the oncoming flow. The connection points are shown below in Figure 10. The load cells were connected to the port and starboard side of the barge via a rope connection point.

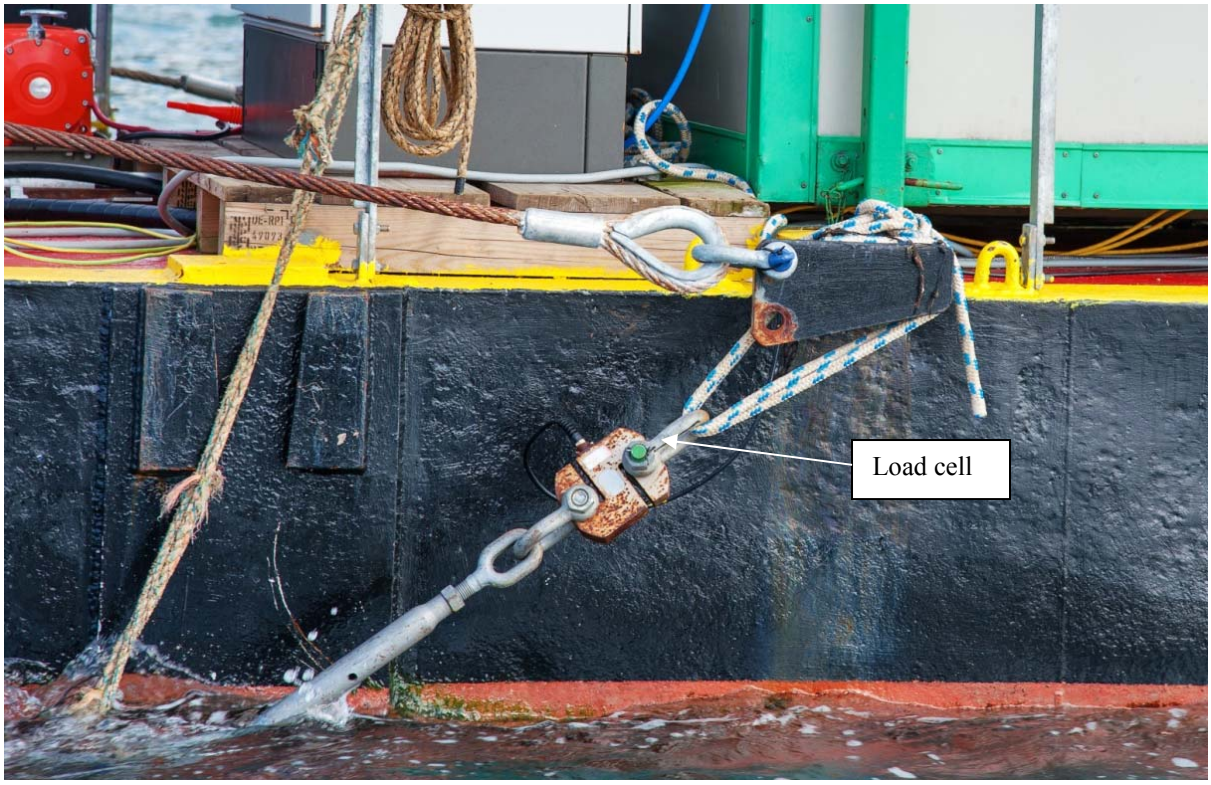

Figure 10: Load cell mounted on starboard side connected to turbine support frame

Mounted on the bow of the barge were an ADP (2), a Differential GPS (DGPS, 4) and mounted on the starboard side of the bow were connection points for a second ADP, a Nortek Vector Acoustic Doppler Velocimeter (ADV, 3) and a Rockland Scientific MicroRider.

The incoming flow conditions were measured using the ADP mounted on the barge bow, at 10m, approximately 2.5D_E (turbine diameters), directly upstream from the turbine centreline (to IEC recommendation, Subclause 7.2). The recorded velocity was split into bins; the bin size of the ADP was 0.2m, so that there were 20 bins covering the rotor area. Due to the beam spread of 25° of the ADP, the velocity is averaged over an area of 3.17m diameter at rotor midheight, which will give an approximate value over most of the rotor area. The power weighted velocity across the projected capture area was calculated and used for quantifying the inflow conditions.

A second ADP was mounted along the starboard side, at 2.25D_E upstream of the turbine, but with over 0.5D_E lateral offset. This was used to determine the importance of the location of the velocity measurement for testing the turbine performance.

The DGPS was used to record the position of the barge during operation, to determine if there was any drift or excessive swing about the mooring. The second ADP, ADV and MicroRider on the starboard side were deployed for one week to measure the inflow turbulence and compare the effectiveness for each instrument type in inflow characterisation; these results will be published separately. Below, in Table 2, is a summary of the equipment used during this deployment.

The data was collected using a Compact RIO and Labview system. The data was collected at 10Hz (except the ADP which was 1Hz) and the turbine, load cell and velocity measurements were synchronised. The uncertainties of each measured parameter used in subsequent analysis in this paper are detailed below in Table 3.

Table 2: Summary of sensors in data acquisition

Instrument	Manufacturer	Mounting	Measurement	Data Frequency	Characteristic
Speed transducer	VS Sensorik	Drive shaft	RPM	10Hz	Speed of turbine Tip Speed Ratio
Inverter	Schneider	Cabinet	Electrical power Voltage Electrical current	10Hz	Generated power Power performance Voltage Electrical current
Load cell	Althen	Port and starboard sides	Load	10Hz	Thrust on support frame and turbine Thrust performance
Aquadopp ADP	Nortek	Support frame Bow centreline Starboard bow	Wake velocity Inflow velocity Inflow velocity	1Hz	Wake Power weighted inflow Power performance Turbulence comparison
Vector ADV	Nortek	Starboard bow	Point velocity	64Hz	Turbulence comparison
MicroRider	Rockland Scientific	Starboard bow	Turbulence	2056Hz	Turbulence comparison
Downscan Sonar	Lowrance	Starboard bow	Depth Incoming bodies	-	Bottom tracking Mammal recording

Table 3: Measured uncertainties

Measured parameter	Uncertainty component	Error
Electric Power	Current transformers	±3.3A
	Variability of electric power	±3000W
Thrust	Load cell	<0.03% of end value (3ton)
Current Speed	Current profiler accuracy	1% of measured value ±0.5cm/s
	Depth measurement relative to performance surface	±1cm (fixed brackets)
	Misalignment of performance surface with principal flow direction	±5° (by sight)

4.4 Operating conditions

There are several constraints on testing in a tidal field environment. Firstly, as described previously, there is only sufficient flow speed on the flood tide at the site, so flood-only operation was employed. The flood runs for two cycles of approximately 6 hours per day. At this site operation is only during daylight hours, so only one flood cycle could be tested, which led to 6 testing hours each day (provided the testing period was during daylight hours). 48 days of testing over a 6 hour tide were conducted, which gave 288 hours of operation.

4.5 Environmental Monitoring

During operation there were several aspects of environmental monitoring. Firstly the barge had a sonar unit (3 in Figure 5) mounted on the bow to record the depth and any incoming mammals, fish or flora. The sonar recorded the flow $2.5D_E$ upstream from the turbine, so any potential collisions could be avoided by applying an electrical brake to the turbine. During operation there was always at least one person on the barge to monitor the turbine and to conduct mammal surveying. There was a full 360° survey of the surrounding area every 15 minutes to check for mammals. Any sightings were recorded and a shut-down exclusion zone of 50m (visual) was implemented. An electrical brake was applied during shut-down. During the testing period there were 29 mammal sightings and 6 shut-down events. There is no evidence to suggest that mammals were harmed during the testing of the tidal turbine.

5. Results

5.1 Data post-processing

The data was collected synchronously at 10Hz for the turbine, load cells and at 1Hz for the inflow velocity. All post-processing was applied to data as per IEC technical specification [12, Section 9]; further detail and equations can be found in the reference document, though key equations will be presented here. No data filtering is permissible in the IEC standards [12, Clause 9.2.1]. The inflow velocity, denoted in later graphs as U_{in}, was power-weighted across the rotor plane [12, Clause 9.3 - 9.7], as shown in Equations 1-7:

$$\widehat{U}_{i,j,k} = \left[\frac{1}{A} \cdot \sum_{k=1}^{s} U_{i,j,k,n}^{3} \cdot A_k\right]^{1/3} \quad (1)$$

where A is the total projected capture area in m^2 of the tidal energy converter;
A_k is the area in m^2 of the k^{th} current profiler bin through the projected capture area;
s is the total number of current profiler bins normal to the principal axis of energy capture across the projected capture area;
i is the subscript number defining the velocity bin number;
j is the subscript number of a time instant when the measurement is performed;
k is the subscript number of the current profiler bin;
n is the subscript number defining an individual data point in velocity bin i;

306 $U_{i,j,k,n}$ is the magnitude tidal current velocity in m/s flowing through the k^{th} current
307 profiler bin of the projected capture area.

308 The power weighted velocity was used for the assessment of instantaneous output power, but
309 the velocity, power and efficiency were binned by velocity. The mean bin equations for
310 velocity and active electrical power are given below:

$$\overline{U}_{i,n} = \left[\frac{1}{L} \cdot \sum_{j=1}^{L} \widehat{U}_{i,j,n}{}^{3}\right]^{1/3} \tag{2}$$

$$\bar{P}_{i,n} = \left[\frac{1}{L} \cdot \sum_{j=1}^{L} P_{i,j,n}{}^{3}\right]^{1/3} \tag{3}$$

$$\overline{U}_i = \frac{1}{N_i} \cdot \sum_{n=1}^{N_i} \overline{U}_{i,n} \tag{3}$$

$$\bar{P}_i = \frac{1}{N_i} \cdot \sum_{n=1}^{N_i} \bar{P}_{i,n} \tag{4}$$

311

312 where N_i is the number of data points in velocity bin *i;*
313 $\bar{P}_i$ is the mean recorded TEC power output in W in the i^{th} velocity bin, denoted in later
314 graphs and text as P_{el};
315 $\overline{U}_i$ is the mean current velocity in m/s in the i^{th} velocity bin.

316 The vertical shear profile is also determined from the velocity data as described below:

$$\overline{Ushear}_{i,k,n} = \frac{1}{L} \cdot \sum_{j=1}^{L} U_{i,j,k,n} \tag{5}$$

$$\overline{\overline{Ushear}}_{i,k} = \frac{1}{N_k} \cdot \sum_{n=1}^{N_k} \overline{Ushear}_{i,k,n} \tag{6}$$

317

318 where $U_{i,j,k,n}$ is the magnitude of tidal current velocity flowing through the k^{th} current profiler
319 bin, as defined in equation (1);
320 L is the number of data samples in the defined averaging period which produces data
321 point n;
322 $\overline{Ushear}_{i,k,n}$ is the mean current velocity data point flowing through current profiler
323 bin k over a given averaging period at a specific velocity increment, i;
324 N_k is the number of data points in current profiler bin k;
325 $\overline{\overline{Ushear}}_{i,k}$ is the mean recorded current velocity at current profiler bin k in the i^{th}
326 velocity bin.

327

The TEC efficiency was also determined, using the following formula:

$$\eta_{system,i} = \frac{\overline{P_i}}{\frac{1}{2} \cdot \rho \cdot A \cdot \overline{U_i^3}} \quad (7)$$

where A is the total projected capture area in m^2 of the tidal energy converter;
$\eta_{system,i}$ is the TEC overall efficiency in the i^{th} current velocity bin;
$\overline{U_i}$ is the mean velocity in m/s of the tidal current in current velocity bin i
$\overline{P_i}$ is the recorded electrical power output in W in current velocity bin i, denoted in later graphs and text as P_{el};
ρ is the fluid density in kg/m^3, as defined in Subclause 9.1.1.

The load cell values were corrected for frame drag (measured in tests with no turbine blades attached) and the angle of the connecting wires to derive turbine thrust. Time series results were produced using the raw data and the time-averaged data sets were averaged as per [12, Clause 8.6]. The IEC suggests using an averaging period between 2 and 10 minutes; the data presented here has been 4min averaged. 4 minute averages were found, in [5], to remove instantaneous data noise and provide consistent vertical flow profiles, so are suitable for data analysis purposes.

5.2 Rotor shear profile

Given the small diameter of the rotor the shear profile of the channel was not anticipated to affect the velocities across the capture area. Figure 11 shows the variation of the velocity across the rotor depth for 7 data sets.

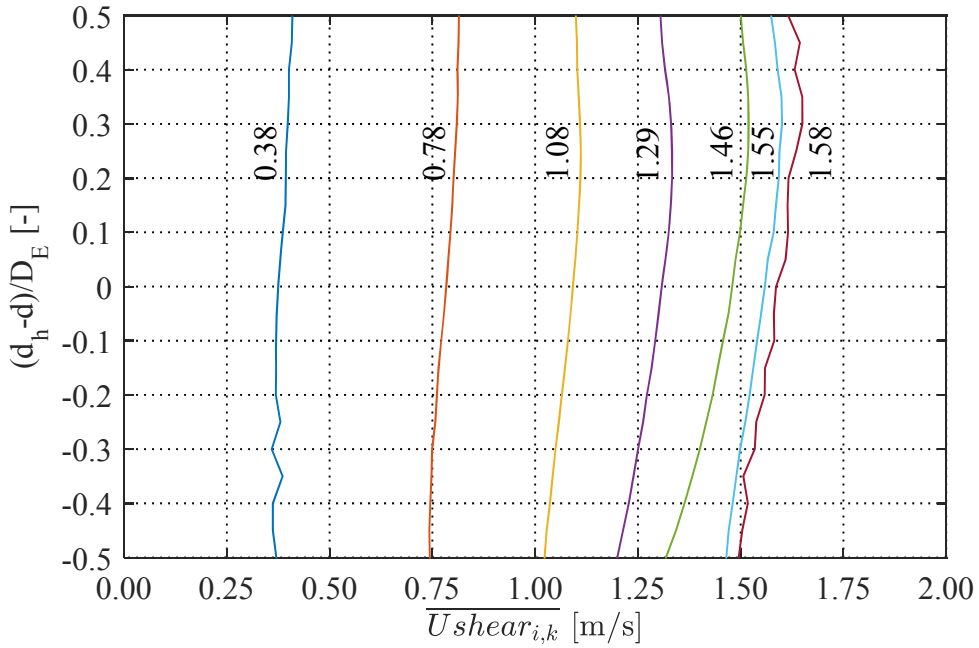

Figure 11: Shear velocity profiles across rotor depth

These represent the streamwise velocity across the 20 bins covering the rotor at banded velocities (as described in the equations above), with the power-weighted velocity given. A shear profile develops over the rotor area, with the shear typically becoming more pronounced with velocity. The difference between the lowest velocity, at the greater depth, and the power-weighted velocity is minimal. The average difference between the velocity at the lowest blade tip and the power-weighted velocity is 0.07m/s. This small variation is only 3.5% of the rated power.

5.3 Time series results

The variations in the inflow velocity, electrical power, thrust, rotational speed and barge pitch during one flood cycle, on the 12th July 2014, are shown below in Figure 11. These use 10s moving averages to show the variation with time.

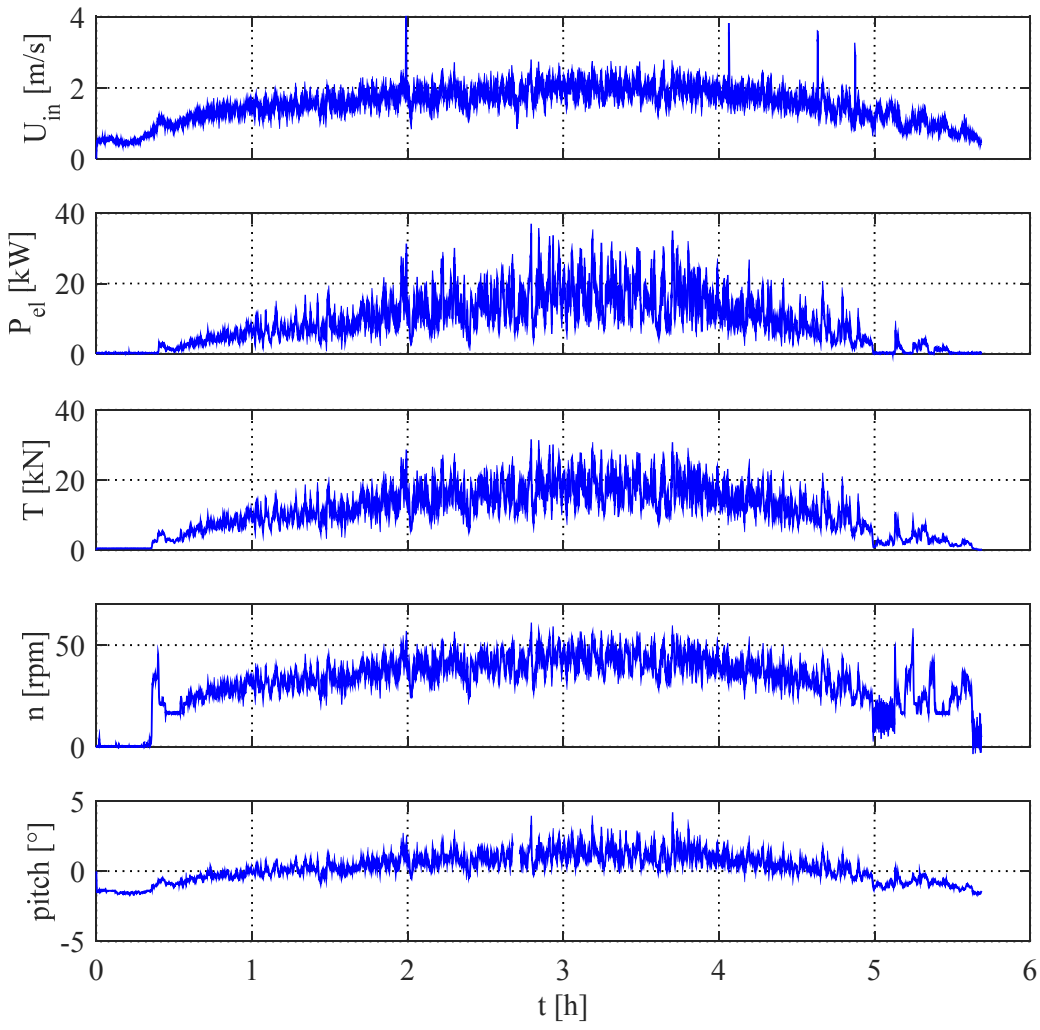

Figure 12: Exemplary time series (12th July 2014)

The velocity can be seen to increase with time, until peak flood after 3 hours, then to decelerate until high water. Maximum flow occurs over a period of approximately 2 hours, though during this time the velocity can vary by up to ±0.5m/s, from 1.5m/s to 2.5m/s, which is 25% of the mean velocity.

The fluctuation in velocity appears to influence the other parameters, particularly the electrical power. The maximum fluctuation of the electrical power occurs at the instance of maximum flow, with power variations of ±10kW, or 50% of the mean power. The fluctuation in power could result in differences from that predicted for the mean flow speed in steady state tests. The cut-in of the electrical power also occurs when there is a gust in the flow speed after approximately 25mins into the tide. This leads to cut-in velocity being exceeded and the power control starts. This gust that causes cut-in to be achieved is evident in the turbine RPM which shows a large acceleration in the rotational speed, until the control mechanism activates, reducing the shaft velocity due to the resistive load. Towards the end of the cycle, after 5 hours, the flow speed oscillates about the cut-in speed. This leads to short periods of high RPM when the PTO has not started, alternated with periods of lower RPM where power is produced, until the flow drops to a level where the turbine stops turning.

The thrust follows the same trend as the power, as the turbine is stopped, free turning, or operational. As flow and power increases, the thrust also increases. At maximum flow the variation in thrust is approximately 30% of the mean thrust, so is less significantly affected by the variation in flow than the power output. Particularly clear is the relationship between the power and the thrust during the last hour of the cycle. When the flow is below cut-in and the power is low, the thrust is also significantly reduced. The thrust on the frame and the turbine also result in the barge pitching. When there is no thrust on the structure the barge pitches at -2° and as the flow, and therefore thrust, increases the barge pitches forward up to +3°. Since the ADP is attached to the same barge as the turbine, the pitch of the ADP is the same as that experienced by the turbine, so the correct inflow is recorded. Plus, the effective velocity in the streamwise plane is very similar to that experienced by the ADP/turbine because the pitch angles are so small, so no flow direction correction is applied.

The velocity fluctuations, that influence the other turbine parameters, can be quantified in terms of turbulence intensity, *TI*. This is defined as the fluctuating part of the velocity divided by the mean velocity:

$$TI = \frac{U_{in}{}'}{\overline{U_{in}}} \tag{8}$$

The turbulence intensity at hub height for each data set within each velocity band was calculated and the mean turbulence intensities at each velocity are shown in Figure 13. The turbulence intensity can be seen to decrease with velocity, indicating that the fluctuations about the mean reduce with velocity. The maximum *TI* of 58% occurs at flow speeds of approximately 0.5m/s, so below cut-in speed. At cut-in speed the *TI* is approximately 40%, which reduces down to 17% at 2.1m/s. These large fluctuations in the incoming flow are inherent for tidal flows and are a consideration for device developers. Higher turbulence intensities could cause fatigue to the blades and affect performance, whereas lower turbulence intensities hinder wake recovery downstream from a turbine. Further investigation is required at all of the operational speeds to determine which turbulence intensities affect which turbine parameters, whether performance or fatigue related. Further analysis of the

flow characteristics and the site measured using the ADP and MicroRider data at the test site are presented in [16]; this gives an example of the conditions experienced at the test location.

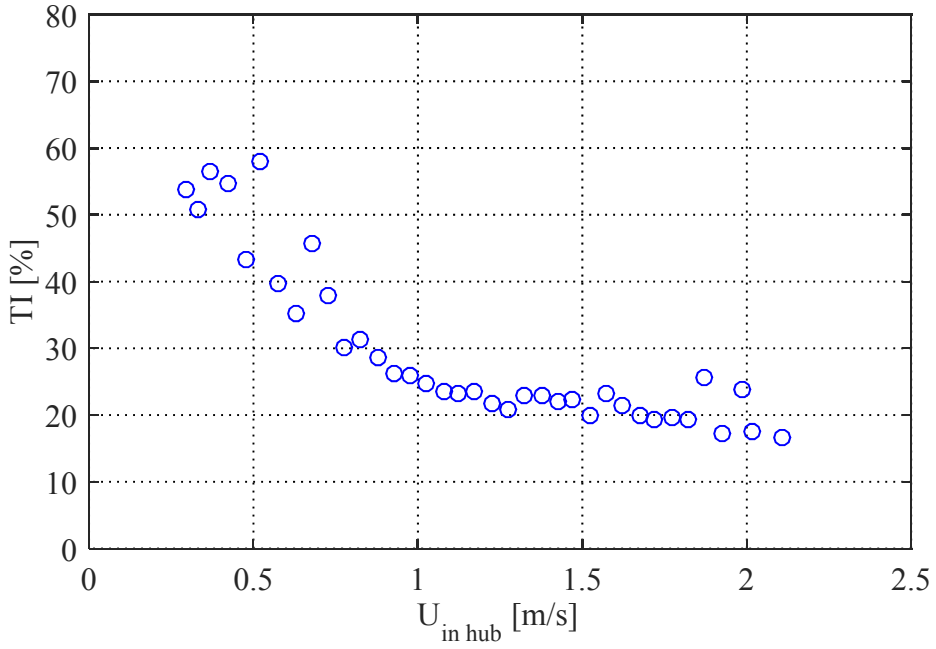

Figure 13: Turbulence intensity at hub height for varying inflow velocities

5.4 Time-averaged performance characteristics

The data for all of the testing period were 4min time-averaged. The resulting maximum, minimum, mean and standard deviation of the recorded TEC power, P_{el}, are shown in Figure 14, plotted against the mean power-weighted inflow velocity (as per [12], Clause 10.7).

The results show that as the velocity increases the power increases exponentially, according to the power curve. This curve follows the same trend as experienced in field pushing tests [11], with cut-in power at approximately 0.8m/s and approximately 18kW at 2m/s. The variation in the results, i.e. between max and min, increases with velocity, potentially due to the variation shown in Figure 12. The mean results are, however, consistent with those predicted from previous tests [11]. The standard deviation in the results is expected to increase until rated power is achieved; however, the rated inflow velocity for the STG turbine is 2.75m/s, which is not reached in these tests.

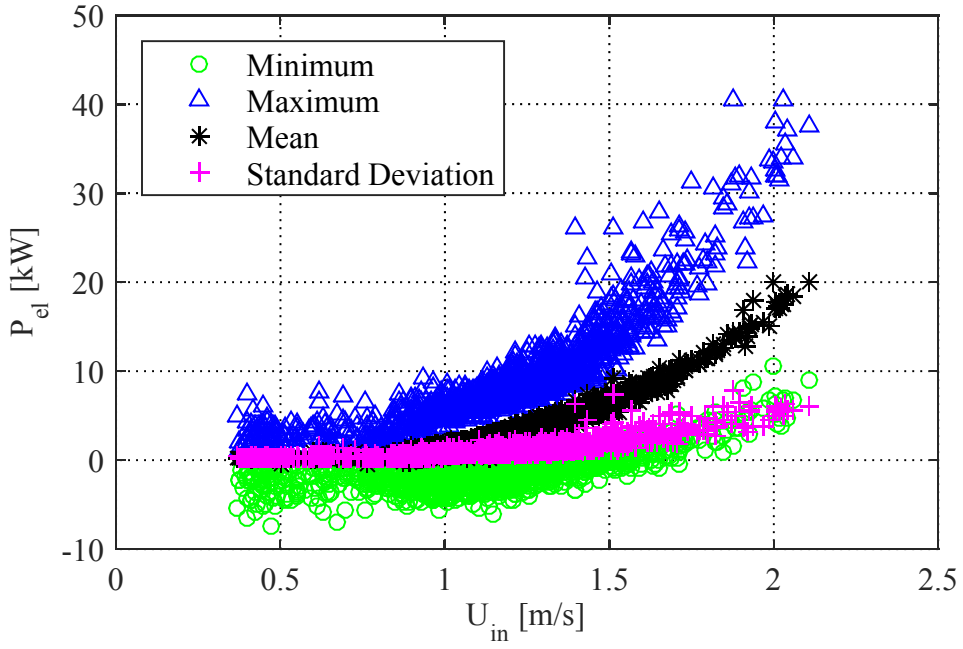

Figure 14: Scatter plot of electrical power output data

The power results were separated into bins, as per [12, Clauses 9.3.1 and 10.8], and the mean recorded TEC power for each velocity bin is shown in Figure 15. This again shows the cut-in at 0.8m/s and the exponential increase in power with velocity. The maximum mean power achieved in these tests, using 4min averages, was 19kW at 2.05-2.1m/s.

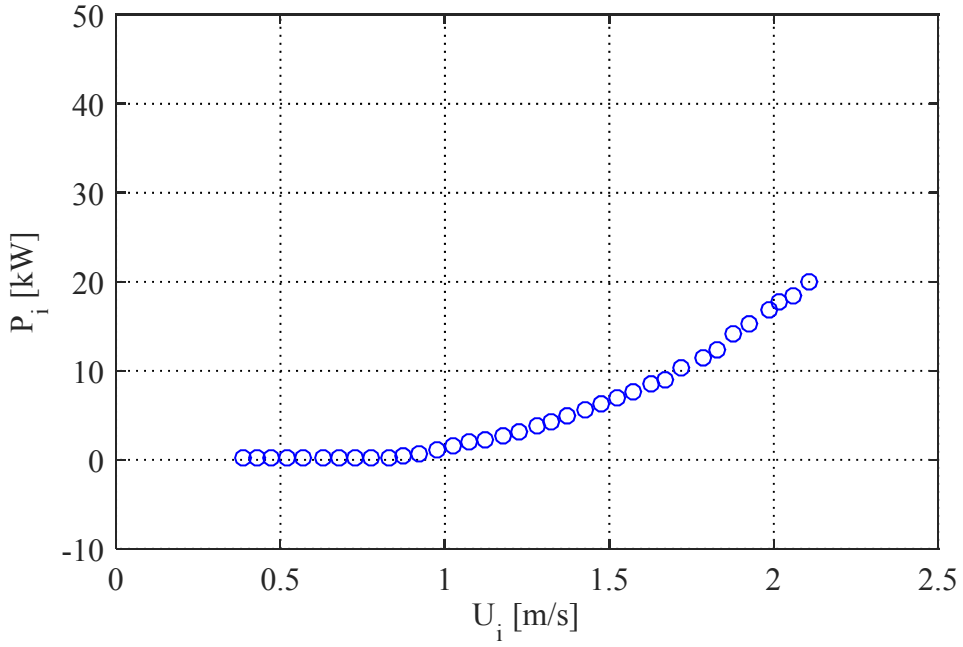

Figure 15: Mean electrical power output for each velocity bin

The overall TEC efficiency was calculated from the recorded electrical power. The efficiency at varying inflow velocities is shown in Figure 16 (as per [12] Clause 10.9). Below cut-in the efficiency is zero, but this increases with velocity. Above 1.2m/s the rate of improvement of

efficiency decreases and above 1.5m/s the efficiency begins to plateau. Maximum efficiency is expected at rated power; however, this could not be tested here since the maximum velocities are limited at the current test site. For this data range maximum efficiency was 34%.

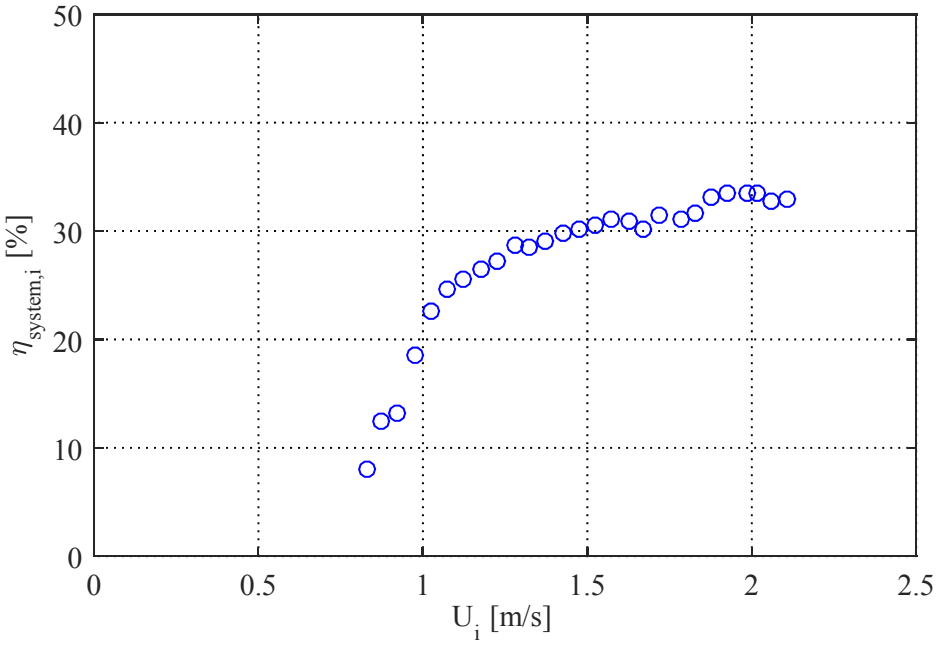

Figure 16: TEC overall efficiency curve

The thrust acting on the support strut and turbine were recorded. The thrust on the turbine only, corrected for load angle and parasitic drag of the frame, against inflow velocity is shown in Figure 17. The mean binned data, similar to that for power in Figure 15, is shown in Figure 18. The thrust experiences a quadratic increase with velocity, as shown in [11].

The thrust on the turbine before cut-in is low, at approximately 0.5kN. At maximum flow speed between 2.05m/s and 2.1m/s the thrust acting on the turbine has increased to 17kN. This is consistent with the results from steady pushing tests [11], though the considerable amount of scatter in the steady tests leaves a margin of error

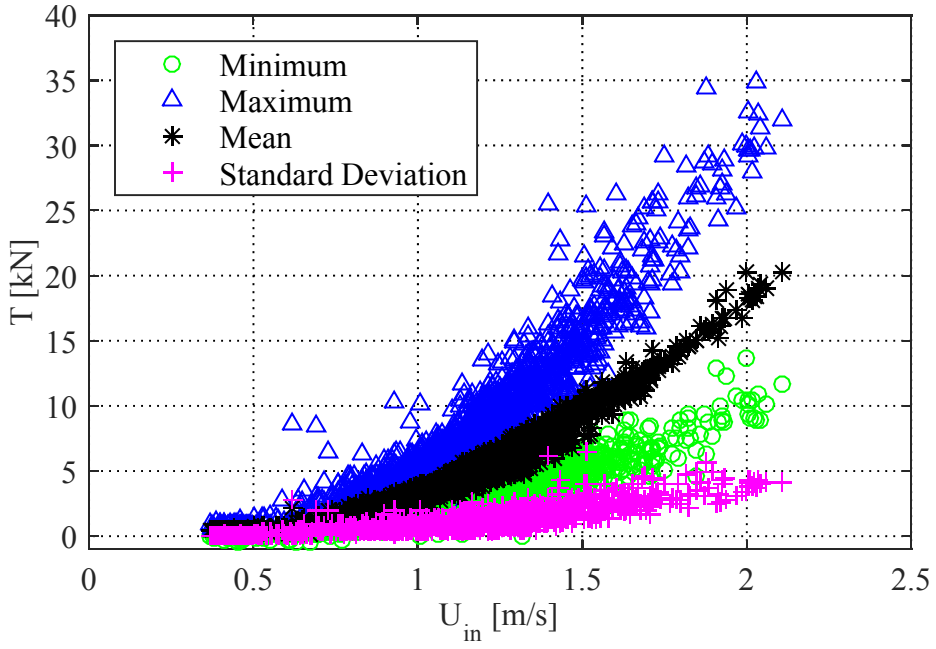

446

447

Figure 17: Scatter plot of thrust data

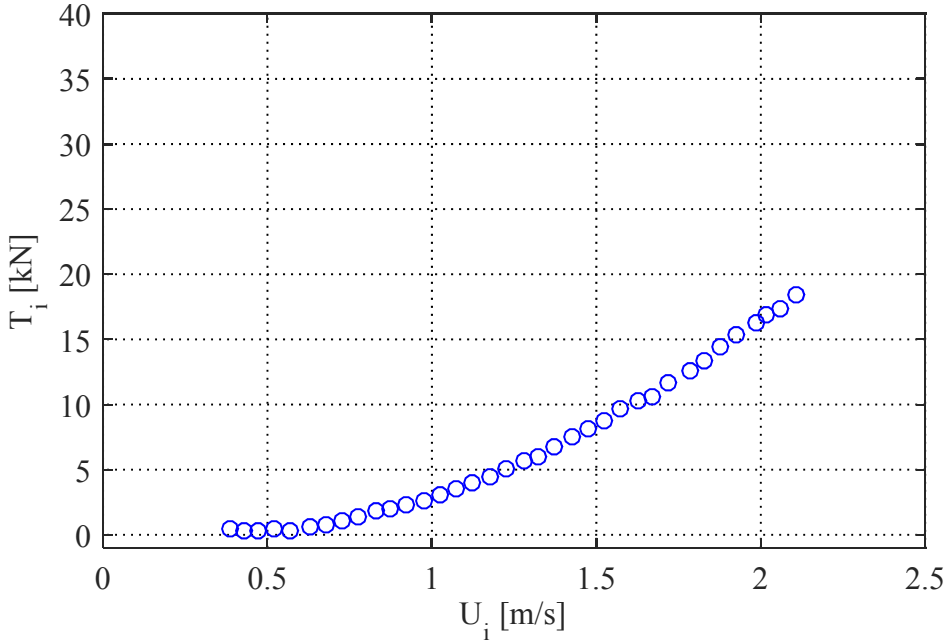

448

449

Figure 18: Mean thrust for each velocity bin

450

6. Conclusions

Full-scale testing of the SCHOTTEL STG turbine has been undertaken at QUB's tidal test facility over a 4 month period in 2014. The key objective of the testing program was to test the full-scale turbine in real, tidal field flows. The key objectives of this paper are: to present a vessel-mounted testing method for field studies of medium- and full-scale tidal devices; to investigate the performance of a full-scale device in tidal flows; and to apply the IEC standards to data processing.

The tests were conducted in the QUB site, during flood, daylight hours for 48 days of testing, to collect 288 hours of data. The 4m, 50kW SCHOTTEL STG turbine was tested in flows between 0 and 2.5m/s, to achieve time-averaged electrical power output up to 19kW. The testing method was therefore appropriate for testing a full-scale device at these flow speeds.

During the testing the turbine RPM, torque, mechanical power, electrical power and thrust were recorded. Simultaneously, the inflow velocity, turbulence (measured with 3 different instruments) and wake velocities were also recorded. The location, depth and mammal activity were also tracked. All the data was recorded and processed according to the IEC standards [12, Section 9].

The velocity, power, thrust and pitch curves produced were as expected, both time-varying and time-averaged. The fluctuations at maximum flow recorded were up to 25% of the mean for the velocity, 50% for the electrical power and 30% for the thrust, showing significant variation of inflow conditions during testing. The maximum turbulence intensity recorded was approximately 58%, though in the turbine operational range was between 40% and 17%. The barge pitch during a testing cycle could vary up to 5° as well. The maximum mean electrical power achieved during the entire testing period was 19kW in flow speeds between 2.05 and 2.1m/s. TEC efficiency reached 35% at 2.0-2.05m/s. In the velocity range tested, as velocity increased so did power production and power efficiency, which also corresponded with reducing turbulence efficiency. The thrust was approximately 0.5kN when the turbine had not cut in, and reached 17kN in maximum flow. The data was all assessed to IEC standards.

During the testing campaign there were many more data sets collected, including turbulence and wake measurements. These will be analysed and published in due course. Further tests may include higher flow speed tests in similar flow, to reach rated velocity and power.

Acknowledgements

The author's would like to acknowledge the funding granted by the EU for the MaRINET Access Program which allowed this work to be conducted. They would also like to acknowledge the funding granted by Invest Northern Ireland for the TTT2 project that supported this work. Many thanks also to the subcontractors and partners who worked on this project: Cuan Marine Services, ARR Ltd, Fraunhofer IWES, Oceanflow Energy, Joules Energy Efficiency, McLaughlin and Harvey and the staff and students at both SCHOTTEL and QUB.

References

[1] ScotRenewables scale model testing, http://www.scotrenewables.com/technology-development/scale-model-testing Accessed 6th Oct 2014

[2] Oceanflow scale model testing. http://www.oceanflowenergy.com/development-status.html Accessed 6th Oct 2014

[3] Andritz Hydro Hammerfest tidal testing, http://www.hammerfeststrom.com/products/tidal-turbines/hs1000/ Accessed 6th Oct 2014

[4] Alstom TGL tidal testing, http://www.alstom.com/products-services/product-catalogue/power-generation/renewable-energy/ocean-energy/tidal-energy/tidal-power/ Accessed 6th Oct 2014

[5] G. Savidge, D. Ainsowrth, S. Bearhop, N. Christen, B. Elsaesser, F. Fortune, R. Inger, R. Knnedy, A. McRobert, K.E. Plummer, D. Pritchard, C.E. Sparling, T. Whittaker, Marine Renewable Energy Technology and Environmental Interactions, M.A. Shields and A. Payne (eds.), Springer

[6] Verdant Power KHPS tidal testing, http://www.verdantpower.com/kinetic-hydropower-system.html Accessed 24th March 2015

[7] Atlantis Resources AR1000 tidal testing, http://atlantisresourcesltd.com/turbines/ar-series/ar1000.html Accessed 24th March 2015

[8] Scotrenewables tidal testing. http://www.scotrenewables.com/250kw-prototype/sr250-testing Accessed 6th Oct 2014

[9] L. Luznik, K.A. Flack, E.E. Lust, D.P. Baxter, Hydrodynamic performance of a horizontal axis tidal turbine under steady flow conditions, Paper presented at Oceans, Hampton Roads VA, 14-19 Oct 2012.

[10] P. Jeffcoate, B. Elsaesser, T. Whittaker, Testing tidal turbines - Part I: Steady towing tests vs. Tidal Mooring Tests, Paper presented at ASRANet, Glasgow, UK, 15-17 Sept 2014.

[11] R. Starzmann, M. Baldus, E. Groh, N. Hirsch, N.A. Lange, S. Scholl, Full-Scale Testing of a Tidal Energy Converter Using a Tug Boat, Paper presented at EWTEC, Aalborg, Denmark, 2-5 Sept 2013.

[12] IEC/TS 62600-200. Marine energy – Wave, tidal and other water current converters – Part 200: Electricity producing tidal energy converters – Power performance assessment

[13] C.B. Boake, M. Atcheson, T.J.T. Whittaker, I.G. Bryden, Selection of a large model scale field wave and tidal test site in Strangford Lough, UK, 1st International Conference on Sustainable Power Generation and Supply (SUPERGEN) (2009) pp. 7

[14] R. Nicholls-Lee, Adaptive Composite Blades for Horizontal Axis Turbines, PhD thesis, University of Southampton, 2011

525 [15] R. Starzmann, M. Baldus, E. Groh, N. Hirsch, N.A. Lange, S. Scholl, A Stepwise
526 approach towards the development and full-scale testing of a marine hydrokinetic turbine,
527 Proceedings of the 1st Marine Energy Technology Symposium (METS13), April 10-11,
528 2013, Washington, D.C.

529 [16] H. Torrens-Spence, P. Schmitt, P. Mackinnon, B. Elsaesser, Current and Turbulence
530 Measurement with Collocated ADP and Turbulence Profiler Data, Presented at IEEE/OES
531 11th Current, Wave and Turbulence Measurement Workshop, March 2-6, 2015, Florida, USA.